Stabilizing Role of Calcium Store-Dependent Plasma Membrane Calcium Channels in Action-Potential Firing and Intracellular Calcium Oscillations

J. M. A. M. Kusters,* M. M. Dernison,[†] W. P. M. van Meerwijk,[†] D. L. Ypey,[†‡] A. P. R. Theuvenet,[†] and C. C. A. M. Gielen*

*Department of Medical Physics and Biophysics, and [†]Department of Cell Biology, Institute for Neuroscience, Radboud University Nijmegen, Nijmegen, The Netherlands; and [‡]Department of Physiology, Leiden University Medical Center, Leiden, The Netherlands

ABSTRACT   In many biological systems, cells display spontaneous calcium oscillations (CaOs) and repetitive action-potential firing. These phenomena have been described separately by models for intracellular inositol trisphosphate (IP_3)-mediated CaOs and for plasma membrane excitability. In this study, we present an integrated model that combines an excitable membrane with an IP_3-mediated intracellular calcium oscillator. The IP_3 receptor is described as an endoplasmic reticulum (ER) calcium channel with open and close probabilities that depend on the cytoplasmic concentration of IP_3 and Ca^{2+}. We show that simply combining this ER model for intracellular CaOs with a model for membrane excitability of normal rat kidney (NRK) fibroblasts leads to instability of intracellular calcium dynamics. To ensure stable long-term periodic firing of action potentials and CaOs, it is essential to incorporate calcium transporters controlled by feedback of the ER store filling, for example, store-operated calcium channels in the plasma membrane. For low IP_3 concentrations, our integrated NRK cell model is at rest at -70 mV. For higher IP_3 concentrations, the CaOs become activated and trigger repetitive firing of action potentials. At high IP_3 concentrations, the basal intracellular calcium concentration becomes elevated and the cell is depolarized near -20 mV. These predictions are in agreement with the different proliferative states of cultures of NRK fibroblasts. We postulate that the stabilizing role of calcium channels and/or other calcium transporters controlled by feedback from the ER store is essential for any cell in which calcium signaling by intracellular CaOs involves both ER and plasma membrane calcium fluxes.

INTRODUCTION

Many neuronal and non-neuronal systems exhibit synchronized oscillatory behavior in networks of electrically coupled cells. This oscillatory behavior has, typically, a twofold character. Cells can reveal periodic action-potential firing, usually triggered by repeated depolarization of the cell membrane by pacemaker cells in the network, or they can have inositol trisphosphate (IP_3)-mediated intracellular calcium oscillations (for an overview, see (1)). Experimental findings have revealed that some cell types—for example, pituitary gonadotroph cells (2)—can have both, and that these types of oscillation are then coupled in these cells. This can be understood from the fact that in cells containing subthreshold concentrations of IP_3, calcium influx during an action potential can activate the IP_3 receptor, triggering an intracellular calcium oscillation by calcium-induced calcium release (3). The opposite, pacemaking by calcium release from the endoplasmic reticulum (ER), is less frequently observed, but was reported recently in interstitial cells of Cajal (4).

The detailed mechanism underlying action-potential firing by cells has been studied extensively since the pioneering work by Hodgkin and Huxley (5) (for an overview, see (6)) and the role of various ion channels in the plasma membrane

and their dynamics has been studied in great detail. Similarly, the mechanism underlying the IP_3-mediated intracellular oscillations has been studied extensively (for a review of various models, see (7–9)). Some studies included a coupling between intracellular calcium oscillations and action-potential firing (see, e.g., (10–12)), but did not study the implications for the long-term stability of calcium dynamics.

Experimental evidence for stability problems with calcium dynamics comes from data from rat hepatocytes (13), which show repetitive waves or oscillations in the cytoplasmic Ca^{2+}. During these waves, Ca^{2+} is released from the endoplasmic reticulum to the cytoplasmic space and subsequently transported back to the stores and to the extracellular space. Maintenance of these Ca^{2+} signaling mechanisms requires the replenishment of intracellular Ca^{2+} that is transported out of the cell. A related problem was addressed theoretically and experimentally for HEK293 cells by Sneyd et al. (14) who demonstrated that small changes in the Ca^{2+} load in cells with intracellular calcium oscillations can move the cell into or out of oscillatory regimes, resulting in the appearance or disappearance of IP_3-mediated calcium oscillations. These authors presented theoretical and experimental evidence that membrane transport can control intracellular calcium oscillations by controlling the total amount of Ca^{2+} in the cell.

However, the unstable calcium dynamics in cells with intracellular calcium oscillations studied by Sneyd et al. (14) is only one side of the problem. Cells without spontaneous intracellular calcium oscillations in a network with propagating

periodic electrical activity due to pacemaker activity also have a problem with controlling calcium dynamics. This can be understood since every action potential will give rise to an increase of cytosolic calcium, due to influx from extracellular space. This leads to an increase of calcium in the ER due to increased SERCA activity. Repetitive firing, therefore, would lead to accumulation of calcium in the ER up to unrealistic values. Using a detailed model for intracellular calcium dynamics, which takes into account the calcium fluxes through both the plasma and the ER membrane, we show that calcium-store-dependent plasma membrane calcium channels, like store-operated calcium (SOC) channels in the plasma membrane, can control the total amount of calcium in the cell under all conditions.

The mathematical modeling in this study is largely based on and supported by experimental data from normal rat kidney (NRK) fibroblasts. NRK fibroblasts in cell culture exhibit growth-state-dependent changes in their electrophysiological behavior. Cells made quiescent by serum deprivation exhibit a resting membrane potential near -70 mV. Upon subsequent treatment with epidermal growth factor, the cells re-enter the cell cycle, undergo density-dependent growth arrest (contact inhibition) at confluency, and repetitively fire action potentials (APs) that propagate via gap junctions through the entire cellular monolayer and are accompanied by intracellular calcium spiking (15). Treatment of the growth-arrested cells with retinoic acid or TGFβ causes the cells to become phenotypically transformed and to depolarize to ~ -20 mV (16).

The action potential fired by NRK fibroblasts is characterized by a fast depolarizing spike to positive membrane potential values, mediated by an influx of calcium through L-type calcium channels. This phase is followed by a plateau phase, which is mediated by a calcium-activated chloride conductance, after which the cells repolarize to their resting value near -70 mV. Based on an electrophysiological characterization and the use of specific inhibitors, we have previously established that L-type calcium channels, calcium-activated chloride channels, and inwardly rectifying K-channels all contribute to the firing of action potentials by NRK fibroblasts (17). Based on the electrophysiological properties of these various channels, determined by patch-clamp analysis on isolated NRK cells, Torres et al. (18) developed a minimal mathematical model for the cell membrane, which correctly described the shape and the width of the action potentials fired by NRK fibroblasts, but could not explain the spontaneous periodic firing of action potentials as observed in the density-arrested NRK cells.

We have recently found that proliferating NRK fibroblasts secrete prostaglandin (PG)F$_{2\alpha}$ in their culture medium (16). Furthermore, we found that this prostaglandin at submicromolar concentrations induces IP$_3$-dependent intracellular calcium oscillations in quiescent serum-deprived NRK cells via activation of the G-protein-coupled prostanoid FP receptor (19). The frequency of these slow calcium oscillations is on the order of that of spontaneously fired action potentials in density-arrested NRK fibroblasts. The similar timescale of both processes strongly suggests that intracellular calcium oscillations (CaOs) provide the cells with a mechanism for periodic firing of action potentials. We therefore hypothesized that the activity of an IP$_3$-dependent intracellular calcium oscillator, perhaps only in a small subpopulation of cells, triggers the periodic firing of action potentials. These action potentials are then propagated in the remainder of the monolayer, causing transient elevations in intracellular calcium in these cells (20). As a matter of fact, we found that growth media conditioned by density-arrested NRK fibroblasts contain nanomolar concentrations of PGF$_{2\alpha}$, which have been shown sufficient to induce calcium oscillations in quiescent NRK cells (16).

A natural way to understand these observations is to assume that almost all cells can switch between two modes of behavior (pacemaker activity by IP$_3$-mediated calcium oscillations and follower-behavior, where cells initiate action potentials by electrical stimulation of the membrane), dependent upon the agonist concentration (PGF$_{2\alpha}$ concentration) near its membrane. We, therefore, wanted to construct a single model of a NRK cell incorporating both calcium oscillations and action potentials. At elevated PGF$_{2\alpha}$, it should act as a pacemaker by producing CaOs, which initiate action potentials. At low agonist concentrations, it should behave as an electrically excitable cell that displays an action potential followed by calcium-induced calcium release by the IP$_3$ receptor after electrical stimulation. NRK cells do exhibit CaOs for very long periods of time (hours). We can only understand that this is possible when their calcium stores have some form of homeostasis: the content of calcium stores cannot go to zero or to infinity over that period. We therefore wanted to find a suitable set of parameters and channels that allowed our model cell to exhibit stable calcium homeostasis.

In this modeling study, we have investigated the interrelationship between periodic firing of action potentials and intracellular CaOs. It represents a first quantitative approach to understand the two-way coupling between action-potential firing and intracellular calcium oscillations. Our model explains how the increased cytosolic calcium concentration during IP$_3$-mediated calcium oscillations activates the calcium-dependent chloride channels, which in NRK fibroblasts cause a depolarization to the Nernst potential of chloride ions near -20 mV. This depolarization then opens the L-type calcium channels in these cells. The model predicts that the shape of an action potential will be different depending on whether it is triggered by electrical stimulation of the membrane or by IP$_3$-mediated calcium oscillations.

The model also illustrates in detail why simply coupling a model for intracellular IP$_3$-receptor-mediated CaOs to a model for the plasma membrane excitability results in unstable intracellular calcium dynamics. We here show that store-operated calcium (SOC) channels can provide the cells

with a mechanism that enables long-term stable calcium homeostasis. Furthermore, the model predicts that in NRK fibroblasts the induction of intracellular calcium oscillations by $PGF_{2\alpha}$ does not depend on gap-junctional coupling with surrounding cells (21), but is an intrinsic property of an isolated cell. The latter is substantiated experimentally (see Appendix 1).

Like NRK fibroblasts, several other cell types have been shown to fire periodic action potentials, which are related to intracellular calcium oscillations. Therefore, the results of this study are relevant not only for NRK cells, but also for other cell types—such as, for example, the pancreatic β-cells in the islets of Langerhans (22,23) and the interstitial cells of Cajal (4).

MODEL DESCRIPTION

The electrical membrane model

This model is an extended version of a previous model by Torres et al. (18). Torres et al. (18) presented a model to explain the excitable properties of the plasma-membrane of normal rat kidney (NRK) cells, which was largely based on experimental work of Harks et al. (17). The membrane components of our model for action-potential firing included an inwardly rectifying K^+ conductance (G_{Kir}), a small leak conductance (G_{lk}), an L-type calcium conductance ($G_{Ca(L)}$), a cytoplasmic calcium-dependent chloride conductance ($G_{Cl(Ca)}$), and a plasma-membrane calcium (PMCA) pump. In the present model we added a store-operated calcium (SOC) channel and we improved the properties of G_{Kir} and $G_{Ca(L)}$ (see Fig. 1 for a diagram of the full conceptual model).

The general differential equation (Eq. 1; see Appendix 2 for this and all other numbered equations) describing NRK cell excitability is obtained by setting the capacitive membrane current (term left from equation sign) equal to the sum of all conductive currents (all terms at the right). The properties of these currents are defined by Eqs. 2–16. The inward rectifier K^+ conductance, characterized by Eqs. 2–5, shunted by a small leak conductance G_{lk} (Eq. 6), determines the resting membrane potential of the cell near -70 mV. Action potentials are initiated by a depolarization to ~-40 mV, which opens the L-type calcium channel. The L-type calcium current (Eq. 7) is characterized by a Hodgkin-Huxley-type activation parameter m (Eqs. 8–10), an inactivation parameter h (Eqs. 11–13), and an inactivation parameter v_{Ca}, which depends on the calcium concentration in the cytosol (Eq. 14). Opening of the L-type calcium channel causes an inflow of calcium ions and a corresponding depolarization to $\sim+20$ mV. The increased calcium concentration in the cytosol activates the calcium-dependent chloride channels (Eq. 15). This causes a plateau phase at the Nernst potential of the calcium-dependent chloride channel near 20 mV as long as the calcium concentration in the cytosol is elevated (17). Final repolarization to the resting
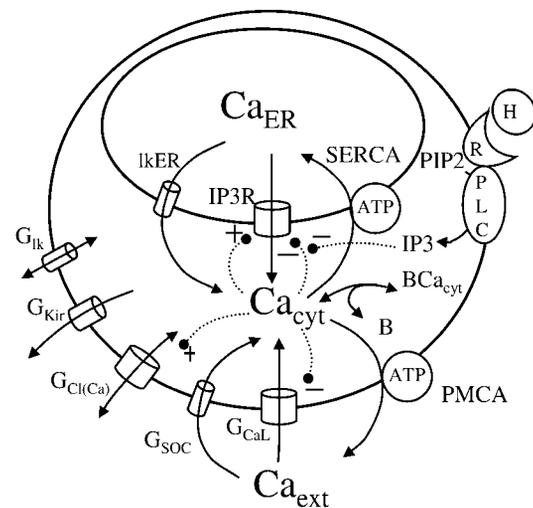

FIGURE 1 Conceptual model of the processes involved in membrane excitability and intracellular calcium oscillation in NRK cells. The model of NRK cell membrane excitability consists of leak channels (see G_{lk}), K_{IR} channels (see G_{Kir}), Cl(Ca)-channels (see $G_{Cl(Ca)}$), SOC channels (see G_{SOC}), L-type Ca-channels (see G_{CaL}), and a PMCA pump. The model for intracellular calcium oscillations consists of a SERCA pump, leak channels through the ER membrane (see $lkER$), and an IP_3 receptor (see IP_3R). The value IP_3 is produced by phospholipase C (PLC) upon binding of a hormone (H) to a plasma membrane receptor (R).

potential results from the removal of intracellular cytoplasmic calcium by the calcium pumps (PMCA), which causes deactivation of the calcium-dependent chloride channel. G_{Kir} then supports repolarization by reactivation. The activity of the PMCA pump increases with the calcium concentration in the cytosol (Eq. 20), in agreement with Caride et al. (25).

In the model by Torres et al. (18), the steady-state parameter of inactivation h_∞ for the L-type calcium channel consisted of a sum of two voltage-dependent components. The first one represented the conventional voltage-gated inactivation process, while the second one was meant to mimic calcium-dependent inactivation. Since recent experiments argue against this second term (26), we simplified the inactivation parameter to a genuine voltage-dependent term in Eq. 12. This allowed us to set half-activation of m_∞ to -15 mV (Eq. 9) in agreement with experimental data of Harks et al. (17) (see their Fig. 3) and to introduce a multiplicative calcium-dependent and V_m-independent inactivation parameter v_{Ca} (Eq. 14) in Eq. 7, as in Bernus et al. (26).

Another modification refers to the K_{IR} channel properties, which, in the model by Torres et al. (18), did not include the effect of variations in external potassium concentration. Since changes in extracellular K-concentration do affect the Nernst potential for the K-ions, we have modified the parameters for the inward rectifier in agreement with ten Tusscher et al. (27) in Eqs. 2–5.

A last modification of the model for the NRK cell membrane by Torres et al. (18) is the addition of a so-called store-operated-calcium (SOC) channel. The existence of

SOC channels is well documented in the literature (28). This channel allows calcium ions to flow from the extracellular space into the cytosol at a rate inversely proportional to the calcium concentration in the ER. This property of the SOC channel is given by Eq. 16. The relevance of the SOC channel for the model will be explained in detail later.

The reaction equations for calcium buffering are described by Eqs. 17 and 18 as in Torres et al. (18). The terms $[B]$ and $[BCa]$ denote the concentration of the buffer and the buffer-calcium complex, respectively, whereas T_B denotes the total fixed concentration of buffer molecules. For the parameter values of the electrical membrane model, see Table 1.

The intracellular calcium dynamics model

In contrast to the membrane model, the calcium oscillator model is a nonelectrical model. It is, so far, common practice to model intracellular calcium oscillations in this way, probably because CaOs seem to result primarily from the calcium- and IP$_3$-dependent properties and not from the voltage-dependent properties of the IP$_3$ receptor. The intracellular calcium oscillator is controlled by the agonist PGF2α ((19), see also Appendix 1). PGF2α diffuses through the extracellular space and binds to the cell-surface receptor, thus activating a G-protein. This, in turn, activates phospholipase C (PLC), producing IP$_3$ from phosphatidylinositol

TABLE 1 Parameter values of the electrical membrane properties, including buffering

C_m*	20	pF
G_{Kir}*	2.2	nS
K_{ost}	5.4	μM
K_o	5.4	μM
K_i*	120	μM
E_{lk}*	0	mV
G_{lk}*	0.05	nS
E_{CaL}*	50	mV
G_{CaL}*	0.7	nS
K_{vCa}	10	μM
$E_{Cl(Ca)}$*	-20	mV
$G_{Cl(Ca)}$*	5	nS
$K_{Cl(Ca)}$	35	μM
G_{SOC}	0.05	nS
E_{SOC}	50	mV
K_{SOC}	10	μM
J_{PMCA}^{max}	1.6×10^{-5}	μmol/(s $\times$ dm^2)
K_{PMCA}	0.25	μM
z_{Ca}	2	
A_{PM}	2×10^{-7}	dm^2
Vol_{cyt}	1×10^{-12}	dm^3
F	96,480	C/mol
R	8.314	m^{2}kg/(s^2 Kmol)
T	293	K
k_{on}	13	(μMs)$^{-1}$
k_{off}	2.28	s^{-1}
T_B	20	μM
Ca$_{ext}$	1800	μM

*Values from Harks et al. (17); other values from Torres et al. (18), except the new parameters (G_{SOC}, K_{SOC}, K_{ost}, and K_o).

bisphosphate. IP$_3$ diffuses through the cytoplasm until it binds to the IP$_3$ receptor on the surface of the ER. For each simulation in this article, we use a fixed IP$_3$ concentration.

The flow of calcium between cytosol and ER is characterized by three fluxes (3): J_{SERCA}, J_{IP_3R}, and J_{lkER} (see Fig. 1). The rate of change of calcium concentration in the cytosol due to inflow from the endoplasmic reticulum (ER) is given by

$$Vol_{cyt}\frac{d\left[Ca_{cyt}^{2+}\right]}{dt} = -Vol_{ER}\frac{d\left[Ca_{ER}^{2+}\right]}{dt}$$
$$= A_{ER}(J_{IP_3R} + J_{lkER} - J_{SERCA})$$

(compare to Eqs. 21 and 22), where A_{ER} represents the size of the surface of the endoplasmic reticulum and Vol_{cyt} and Vol_{ER} represent the cytoplasmic volume and the volume of the ER, respectively. J_{IP_3R} (Eq. 23) is the flux of calcium through the IP$_3$-receptor channel into the cytosol, J_{lkER} is the leak of calcium through the ER into the cytosol (Eq. 24), and J_{SERCA} is the flux of calcium into the ER by the SERCA pump (Eq. 25).

The equation for the IP$_3$ receptor (Eq. 23) is taken from Schuster et al. (7), who presented an overview with two different models for the IP$_3$ receptor. We took the one from Li and Rinzel (29), which is a reduced version of De Young and Keizer (30) and we slightly modified it. The other model is not compatible with experimental data, as will be explained later.

We took the equation for the flux of calcium through the IP$_3$ receptor in Table 1 in Schuster et al. (7), given by $[k_0 + k_1[(R_a[Ca_{cyt}^{2+}]/(K_a + [Ca_{cyt}^{2+}]))]^3]([Ca_{ER}^{2+}] - [Ca_{cyt}^{2+}])$, which translates into our Eq. 23, where k_0 is the leak term J_{lkER} in our model, k_1 is K_{IP_3R}, $[([Ca_{cyt}^{2+}]/(K_a + [Ca_{cyt}^{2+}]))]^3$ corresponds to f_∞^3, and R_a corresponds to our parameter w.

The terms f_∞ and w represent the fraction of open activation and inactivation gates, respectively. $[Ca_{ER}^{2+}] - [Ca_{cyt}^{2+}]$ is the concentration-difference between calcium in the endoplasmic reticulum and the cytosol and provides the driving force. The value K_{IP_3R} is the rate constant per unit area of IP$_3$-receptor-mediated release.

In the model of Li and Rinzel (29), cytosolic calcium and IP$_3$ play a pivotal role in facilitating and inhibiting the opening of the IP$_3$-receptor channel.

The function f_∞ (Eq. 26) describes fast activation by calcium. Since the dynamics of the f-gate is fast relative to other processes (31), we will not include dynamics in that gate. A small amount of calcium in the cytosol will bind to the activation site and will open the IP$_3$ receptor, triggering calcium-induced calcium release and causing a further increase of the calcium concentration in the cytosol.

From Fig. 2 of Mak et al. (32) it is clear that the activation f_∞ of the IP$_3$ receptor is only determined by the calcium concentration in the cytosol and is independent of IP$_3$. Therefore, we modified the expression for the fast activation in Li and Rinzel, given by $([IP_3]/([IP_3]+d1))([Ca_{cyt}^{2+}]/([Ca_{cyt}^{2+}]+d5))$, into Eq. 26. We replaced the constant $d5$ in Li

and Rinzel by the constant K_{fIP_3} and removed the IP_3 dependence. The equation for inactivation of the IP_3 receptor is defined in Li and Rinzel by $((d2([IP_3]+d1)/([IP_3]+d3))$ $d2(([IP_3]+d1)/([IP_3]+d3))+[Ca_{cyt}^{2+}])$, and we changed it into Eq. 28.

The expression for w_∞ reflects that the inactivation of the IP_3 receptor depends on $[IP_3]$ and $[Ca_{cyt}^{2+}]$. This agrees with data in Fig. 2 of Mak and Foskett (33), showing that the inactivation curve depends on $[IP_3]$ and $[Ca^{2+}]$. We follow Li and Rinzel (29) by using a Hill coefficient of 1 for f_∞ and w_∞. The inactivation-constant time of the IP_3 receptor is defined in Li and Rinzel by $(1/a2(d2(([IP_3]+d1)/([IP_3]+d3)+[Ca_{cyt}^{2+}])))$. We changed it into the equivalent expression, Eq. 29. Since we dropped the first term $([IP_3]/([IP_3]+d1))$ in the expression for the fast activation in Li and Rinzel, the parameter $d1$ was set to zero. The constants $d2$ and $d3$ in Li and Rinzel are equal to $K_{w(Ca)}^{-1}$ and K_{wIP_3}, respectively.

The variable w describes a slow inactivation process with time-dependent kinetics and is characterized by Eqs. 27–29. There is ample evidence suggesting that the time required for IP_3-receptor inactivation is slow in comparison to the time required for IP_3-receptor activation (31). This means that an IP_3 receptor can open quickly and can stay open for a considerable amount of time (allowing calcium to leak out), before inactivation by calcium takes place. The time-constant τ_w (Eq. 29) for calcium-dependent (de-)inactivation of the IP_3 receptor is of the order of 20 s (33) and decreases with an increase in $[IP_3]$ and $[Ca_{cyt}^{2+}]$.

Several studies (see, e.g., (31,34,35)) reported evidence that calcium-dependent inactivation is of the order of seconds. The calcium oscillations and spontaneous action potentials in NRK cells have periods in the order of 30–200 s, so there must be a slow component in the oscillation that governs the interval, which is not observed in the studies just mentioned (31,34,35). Unfortunately, there is no agreement as to which set of data better represents the in vivo behavior. It was not our goal to model the detailed kinetics of the IP_3 receptor, but rather to describe our slow NRK calcium oscillations and to understand the influence of these oscillations upon the membrane excitability and vice versa. Therefore, we chose to modify the time constant of the variable w in such a way that it is relatively fast in high $[Ca^{2+}]$ and slow in low $[Ca^{2+}]$, as well as dependent upon $[IP_3]$, as in Mak and Foskett (33). In this way the variable w is a minimal model of a complexity of mechanisms that all keep the IP_3 receptor closed on a longer timescale. Phosphorylation of the IP_3 receptor has been suggested to cause slow calcium oscillations (36). Another possibility might be that slow oscillations in IP_3 concentration determine the slow dynamics of the cellular calcium response (37). However, at the moment there is no experimental evidence yet for these mechanisms in NRK cells.

At the high values of cytosolic calcium reached after a release wave, the inactivated IP_3 receptor remains closed for some time. This allows a decrease of cytosolic calcium by reuptake of calcium into the ER by the SERCA pump and by extrusion out of the cell by the PMCA pump. The equation for the SERCA pump (Eq. 25) is taken from Lytton et al. (38). The flux of the SERCA pump (J_{SERCA}) increases for increasing cytosolic calcium. The flow through the J_{lkER} channel is proportional to the difference in concentration of calcium in the ER and the cytosol (Eq. 24).

The simple intracellular calcium oscillator is coupled to the intracellular calcium buffer described in The Electrical Membrane Model (see above; see also Eq. 18). For an overview of the parameter values used in this study, see Tables 1 and 2. We did not include calcium buffering in the ER, because we have no data on that buffering in our cells and because separate simulations showed that this buffer had little or no effect on cytoplasmic calcium oscillations and AP firing.

The complete single-cell model

If we combine the membrane model with the model for the intracellular calcium dynamics (see Fig. 1), the currents through the membrane are described by the differential equation (Eq. 1). The rate of change for cytosolic calcium concentration is defined by Eq. 21, and the rate of change for the calcium concentration in the ER is defined by Eq. 22. The value J_{PM} (Eq. 19) couples calcium dynamics to the electrical membrane model, whereas $G_{Cl(Ca)}$ does the opposite. The factor $(1/z_{Ca}F)$ is a conversion factor that transforms a current of calcium ions into a calcium flux changing the cytosolic calcium concentration (Eq. 19). Here F is the Faraday constant and z_{Ca} is the valence of calcium ions.

Dynamic properties of the model

In the past, separate models have been proposed for the dynamics of the cell membrane and for the IP_3-related intracellular calcium oscillations. As we will explain, integrating the two models gives some unexpected complexities, which can only be understood if the two separate components have been clarified in detail. Therefore, we will first

TABLE 2 Parameter values of the intracellular calcium dynamics properties

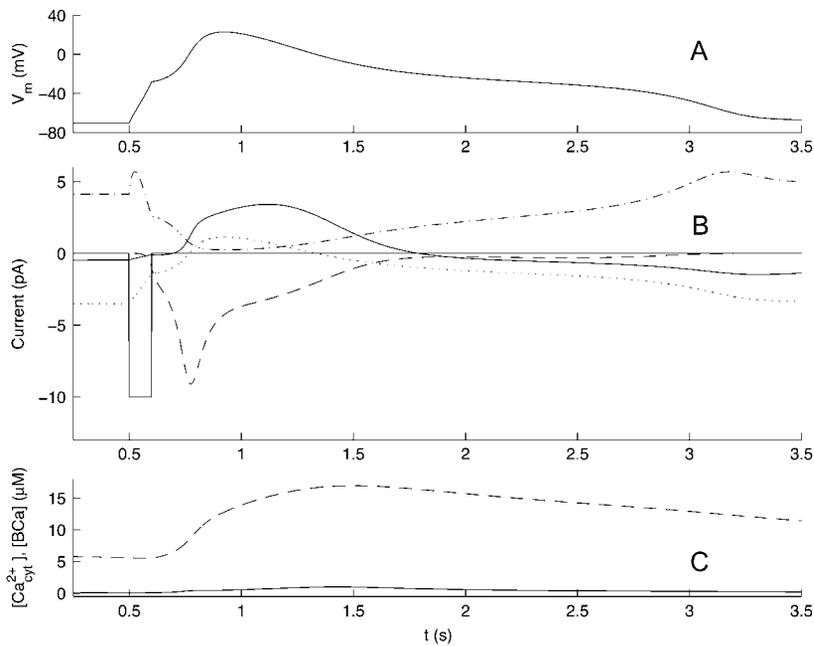|		
A_{PM}	2×10^{-7}	dm^2
Vol_{cyt}	1×10^{-12}	dm^3
A_{ER}	0.3×10^{-7}	dm^2
Vol_{ER}	0.1×10^{-12}	dm^3
K_{lkER}	0.002×10^{-5}	dm/s
J_{SERCA}^{max}	8×10^{-5}	μmol/(s $\times$ dm^2)
K_{SERCA}	0.20	μM
K_{IP_3R}	6×10^{-5}	dm/s
K_{fIP_3}	0.5	μM
$K_{w(Ca)}$	0.5	μM^{-1}
K_{wIP_3}	1.5	μM
a	20	s
k_{on}	13	$(\mu$Ms$)^{-1}$
k_{off}	2.28	s^{-1}
T_B	20	μM

FIGURE 2 Current-clamp simulation in an NRK fibroblast membrane model. Action potential generated upon a current pulse of 10 pA and of 100-ms duration. Panel A shows the simulated membrane potential of the NRK cell model, B shows the currents I_{CaL}(*dashed line*), I_{Kir} (*dash-dotted line*), $I_{Cl(Ca)}$ (*solid line*), I_{lk} (*dotted line*), and the I_{pulse} (*solid line*), and C shows the free (*solid line*) and buffered calcium concentration in the cytosol (*dashed line*). The buffer rates were set to 13 $(\mu Ms)^{-1}$ (k_{on}) and 2.28 s^{-1} (k_{off}). This results in a K_D value of $(k_{off}/k_{on}) = 0.175\ \mu M$. The total buffer concentration T_B was 20 μM. These values were in the same range as reported by Nägerl et al. (39). All parameters were as in Table 1, except for J_{PMCA}^{max}, which was set to the value $4 \times 10^{-5}(\mu M/(s \times dm^2))$ for the electrical membrane model without an IP$_3$-mediated calcium oscillator.

explain the properties of the membrane and intracellular calcium-oscillation models separately, before integrating them into a full model.

Dynamics of the electrical membrane model

Current pulses cause the model to generate action potentials similar to those appearing in real NRK fibroblasts in whole-cell current-clamp experiments. This is illustrated in Fig. 2, which shows the excitable properties of the single-cell model in response to stimulation of the membrane with a current pulse of 10 pA (for parameter values, see Table 1). In response to the current pulse, the membrane potential rises from its resting value near -70 mV to $\sim +20$ mV (Fig. 2 A). The depolarization is caused by the combination of an increasing inward I_{CaL} and a decreasing outward I_{Kir} (Fig. 2 B, *dashed line* and *dashed-dotted line*, respectively). After the initial depolarization to $\sim +20$ mV, a repolarization to ~ -20 mV is caused by inactivation of I_{CaL} and activation of the calcium-dependent chloride channels, which are activated by the increase of cytosolic calcium due to the influx of calcium ions through the L-type calcium channels. The increase of the calcium concentration in the cytosol is shown in Fig. 2 C (*solid line*). The rapid increase of calcium in the cytosol is buffered and decreases due to extrusion by PMCA pump. After inactivation of the L-type calcium channel, the calcium-dependent chloride current (*solid line*, Fig. 2 B) keeps the membrane potential for some time at the plateau phase near -20 mV ($E_{Cl(Ca)}$), which lasts (~ 2 s) until the calcium concentration in the cytosol has decreased to low levels. The calcium-induced $I_{Cl(Ca)}$ goes outward during the peak of the action potential, but reverses into a small inward chloride current during the plateau phase. With the de-

creasing calcium concentration in the cytosol, the conductance of the calcium-dependent chloride channels decreases, and the membrane potential becomes subject to the repolarizing effect of I_{Kir}.

The leak-current I_{lk} follows the shape of the action potential (*dotted line*, Fig. 2 B). The conductance of the SOC-channel in this membrane model has been set to a small constant value (0.05 nS), since it depends on the calcium concentration in the ER, which is not included in the membrane model (I_{SOC} is not shown in Fig. 2, because this current is very small). This leak of calcium ions through the SOC channel is chosen such that the balance between leak through the plasma membrane and extrusion by the PMCA pump gives a cytosolic calcium concentration of 0.08 μM in the steady state at -70 mV. The SOC channel will play an important role when we merge the membrane model with the model for the intracellular calcium oscillator, to make a complete model for the NRK-cell dynamics.

Dynamics of the intracellular calcium oscillator model

When the IP$_3$ concentration is zero, J_{IP_3} equals zero, and the ratio between cytosolic calcium and calcium in the ER is determined by a balance between two fluxes: $J_{SERCA} = J_{lkER}$. Solving this equation for $[Ca_{ER}^{2+}]$ as a function of $[Ca_{cyt}^{2+}]$ gives

$$\left[Ca_{ER}^{2+}\right] = \frac{J_{SERCA}^{max}}{K_{lkER}} \frac{\left[Ca_{cyt}^{2+}\right]^2}{\left[Ca_{cyt}^{2+}\right]^2 + K_{SERCA}^2} + \left[Ca_{cyt}^{2+}\right].$$

Differentiation of this equation gives the rate of change of $[Ca_{ER}^{2+}]$ as a function of $[Ca_{cyt}^{2+}]$,

$$\frac{\partial\left[\mathrm{Ca}_{\mathrm{ER}}^{2+}\right]}{\partial\left[\mathrm{Ca}_{\mathrm{cyt}}^{2+}\right]} = \frac{J_{\mathrm{SERCA}}^{\mathrm{max}}}{K_{\mathrm{lkER}}} \frac{2\left[\mathrm{Ca}_{\mathrm{cyt}}^{2+}\right]K_{\mathrm{SERCA}}^{2}}{\left(\left[\mathrm{Ca}_{\mathrm{cyt}}^{2+}\right]^{2} + K_{\mathrm{SERCA}}^{2}\right)^{2}} + 1.$$

The parameter values of $J_{\mathrm{SERCA}}^{\mathrm{max}}$ and K_{lkER} can be found in Table 2. For low values of $[\mathrm{Ca}_{\mathrm{cyt}}^{2+}]$, $(\partial[\mathrm{Ca}_{\mathrm{ER}}^{2+}]/\partial[\mathrm{Ca}_{\mathrm{cyt}}^{2+}])$ is proportional to $2(J_{\mathrm{SERCA}}^{\mathrm{max}}/K_{\mathrm{lkER}})$, which is ~ 8000. Therefore, when the concentration of cytosolic calcium changes, the concentration of calcium in the ER changes 8000 as much.

In agreement with previous studies (7,29) the behavior of the IP$_3$-receptor system follows that of a Hopf bifurcation. When the concentration of IP$_3$ increases from zero, it reaches a point where spontaneous calcium oscillations occur. This can be understood from Eqs. 26 and 28. For increasing IP$_3$ concentration, the fraction of open inactivation gates (Eq. 28) increases. As a consequence, the leakage of calcium through the IP$_3$ receptor increases and the calcium concentration in the cytosol increases. The fraction of open activation gates (Eq. 26) is independent of the IP$_3$ concentration, but increases when the calcium concentration in the cytosol increases. This provides a positive feedback between the IP$_3$-receptor state and the activation gate: when the IP$_3$ receptor starts leaking calcium, the fraction of open-activation gates increases, contributing to a greater leakage of calcium through the IP$_3$ receptor, and a large burst of calcium will be released through the IP$_3$ receptor.

Fig. 3 A shows the oscillations for an IP$_3$ concentration of 0.5 μM. When the IP$_3$ receptor opens, the calcium concentration in the ER decreases (Fig. 3 A, *middle panel*), whereas the calcium concentration in the cytosol increases (Fig. 3 A, *solid line* in *upper panel*). The buffer absorbs part of the calcium release in the cytosol (*dashed line*, *upper panel*). The lower panel of Fig. 3 A shows the flow through the ER membrane. The flow of calcium ions through the IP$_3$ receptor during the opening of the IP$_3$ receptor is a large, short-lasting flow (*dashed line*). The leak flow is rather small (*solid line*). Integrated over a complete cycle of the IP$_3$ receptor, the flow through the SERCA pump (*dashed-dotted line*) is equal to the flow through the IP$_3$ receptor plus the leak flow.

Increasing the IP$_3$ concentration increases the frequency of the calcium oscillations (compare, in Fig. 3, A (IP$_3$ 0.5 μM) and B (IP$_3$ 1 μM)). The lower panel of Fig. 3 B shows the flows through the ER membrane. The flow of calcium ions through the IP$_3$ receptor during the opening of this receptor shows a large peak, followed by a small shoulder (*dashed line*). The sharp peak in the flow of calcium ions is due to the rapid activation, followed by a fast inactivation of the IP$_3$ receptor. The small shoulder is the result of the slow closing of the f-gate (~ 15 s, related to the slow decrease of cytosolic calcium) and the increase of the difference between calcium in the ER and in the cytosol.

For high IP$_3$ concentrations (IP$_3 > 2\,\mu$M), the oscillations stop at a subcritical Hopf-bifurcation with a hysteresis effect. For these high IP$_3$ concentrations, the IP$_3$ receptor is leaking
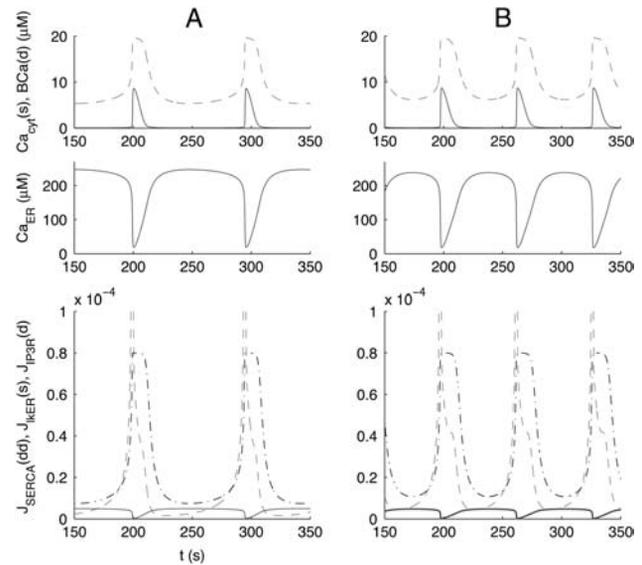

FIGURE 3 Simulation of the intracellular calcium oscillator for an IP$_3$ concentration of 0.5 μM (A) and 1 μM (B). When the IP$_3$ receptor opens, the calcium concentration in the ER decreases (A, *middle panel*), whereas the calcium concentration in the cytosol increases (A, *solid line* in *upper panel*). The buffer absorbs part of the calcium release in the cytosol (*dashed line* in *upper panel*). The lower panel of A shows the flow through the ER membrane. The flow of calcium ions through the IP$_3$ receptor during the opening of the IP$_3$ receptor (*dashed line*), the flow through the SERCA pump (*dashed-dotted line*), and the leak (*solid line*).

continuously, and the f- and w-gates have an open probability near 0.8 and 0.3, respectively, which allows calcium to flow continuously from the ER into the cytosol. The basal calcium concentration in the cytosol remains permanently elevated. This elevated calcium concentration opens the chloride channels in the membrane model, when we couple the intracellular calcium model to the membrane model.

The buffer plays an important role in the model. Increasing the affinity k_{on} of the buffer leads to a frequency decrease of calcium oscillations and a decrease of their peak amplitude. A very large affinity or a very large total buffer capacity reduces the calcium concentration in the cytosol to such an extent that the IP$_3$ receptor will not be activated and calcium oscillations will not occur. Hence, oscillations can only be produced by the model if k_{on} and k_{off} are in the same range. This is achieved by setting $K_{\mathrm{D}} = (k_{\mathrm{off}}/k_{\mathrm{on}}) = 0.175\,\mu$M and $T_{\mathrm{B}} = 20\,\mu$M in agreement with data by Nägerl et al. (39).

Action potentials of the complete cell model evoked by intracellular calcium transients versus external current pulses

In the complete cell model, intracellular calcium oscillations and action-potential firing are coupled. This is illustrated in Fig. 4, which shows the calcium concentration in the cytosol (Fig. 4 A), calcium concentration in the store (Fig. 4 B), and
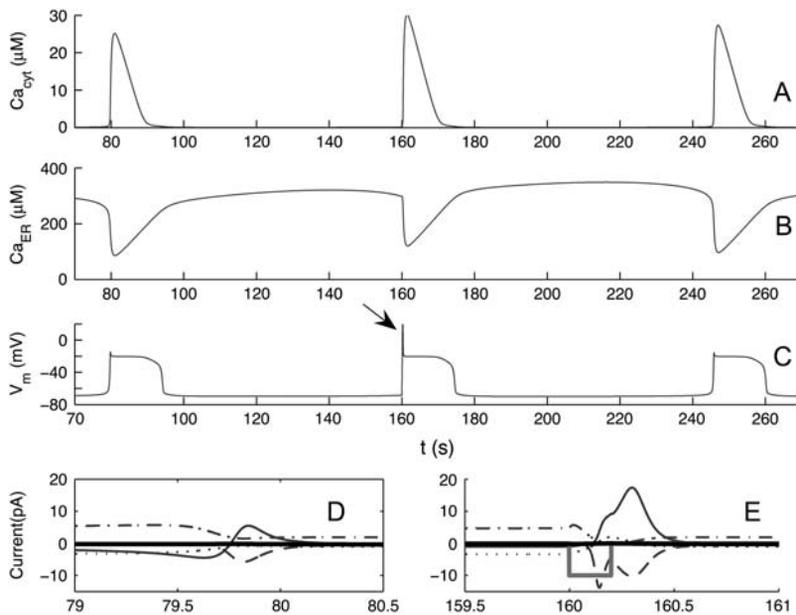
FIGURE 4 Simulation of action potentials (APs) evoked by intracellular calcium transients versus external current pulses in the complete cell model. The figure shows the calcium concentration in the cytosol (*A*), calcium concentration in the store (*B*), and corresponding AP for the complete model with the SOC channel included (*C*), and ion currents I_{CaL} (*dashed line*), I_{Kir} (*dashed-dotted line*), $I_{Cl(Ca)}$ (*solid line*), and I_{lk} (*dotted line*) during a cytosolic calcium transient (*D*, corresponding to the first AP in *C*), and the same ion currents during an external current pulse (*solid line* in *E*, corresponding to the second AP in *C*).

the corresponding action potential (Fig. 4 *C*) for IP$_3$-mediated calcium oscillations (first and last events near times 80 and 240 s) and for electrical stimulation of the membrane (middle event near 160 s). It also shows the ion currents through the membrane for an IP$_3$-mediated calcium oscillation (Fig. 4 *D*) and after an external current pulse (Fig. 4 *E*). At the onset of a calcium cycle during spontaneous calcium oscillations, inflow of calcium from the ER into the cytosol opens the calcium-dependent chloride channel, causing an inward current, i.e., an outward flow of Cl$^-$-ions (*solid line* in Fig. 4 *D*) as long as the membrane potential is below the Cl-Nernst potential near -20 mV, and a corresponding depolarization. The inflow of Ca^{2+} from the ER and the resulting rise of the membrane potential to the Cl-Nernst potential near -20 mV have two opposing effects on the L-type calcium channels. The depolarization causes activation of the L-type calcium channels, but the slow depolarization before reaching the threshold and the increased cytosolic calcium concentration cause inactivation of these channels. The result of these opposing effects is a relatively small inflow of calcium through the membrane, causing a further depolarization above the Nernst potential of the chloride channels, which reverses the current of chloride ions.

Inactivation of the L-type calcium channels after the initial peak of the action potential contributes to repolarization to the Cl-Nernst potential near -20 mV. The reduction of cytosolic calcium by the activity of the SERCA and PMCA pump reduces $I_{Cl(Ca)}$, such that the membrane becomes subject to the repolarizing effect of I_{Kir} (*dashed-dotted line* in Fig. 4 *D*). The role of G_{Kir} in the repolarization results from reactivation of G_{Kir} after deactivation during the upstroke of the action potential. As a consequence, the membrane potential decreases from the voltage plateau near -20 mV to the resting potential near -70 mV.

Fig. 4 *E* shows the ion currents during an action potential (AP) evoked by an external current pulse at time 160 s, just before the expected appearance of an intracellular calcium oscillation. The corresponding AP is shown in Fig. 4 *C* (see *arrow*). It has a much larger initial peak than the intracellular calcium AP. Stimulating the cell with an external current pulse opens the L-type calcium channels, causing a large inward current of calcium ions (*dashed line*). The increase of calcium in the cytosol opens the calcium-dependent chloride channel (*solid line*). Notice that the inward calcium current is approximately three-times-larger than in the case of an AP triggered by an intracellular calcium oscillation (Fig. 4 *D*), which is the reason of the increased AP peak. This difference in the peak between these two types of APs was observed before by Torres et al. (18). Furthermore, the order of onset of calcium- and chloride-ion currents is reversed in both conditions. Inactivation of the L-type calcium channels after the initial peak of the action potential contributes to repolarization to the Cl-Nernst potential near -20 mV. The reduction of the cytosolic calcium by the activity of the SERCA and PMCA pump reduces $I_{Cl(Ca)}$, such that the membrane becomes subject to the repolarizing effect of I_K (*dashed-dotted line*).

The duration of the action potential of the integrated model in Fig. 4 is much longer ($\sim$15 s) than that of the membrane model ($\sim$2 s, see Fig. 2). This is due to the additional presence of the intracellular calcium release mechanism in the ER membrane causing an extended calcium wave and extended opening of Cl(Ca)-channels under the appropriate calcium buffering conditions in the model.

Calcium dynamics stability of the complete cell model

For a steady-state situation without calcium oscillations and without action potentials, solving Eq. 22, so that

$(d[\mathrm{Ca}^{2+}_{\mathrm{ER}}]/dt) = 0$, gives for the balance of the calcium flows into and out of the ER, a steady-state ratio of ~8000 between the concentration of calcium in the ER and cytosol (see Dynamics of the Intracellular Calcium Oscillator Model, above). Similarly, we find for the plasma membrane that the ratio between the calcium concentration in extracellular space (1800 μM) and in the cytosol is determined by the total influx leak of calcium ions through the membrane and the activity of the PMCA pump. For the parameters in our model this ratio is ~30,000 in the steady-state situation in the absence of action-potential firing. Because of these high ratios, small variations in the leak or activity of the pumps cause large changes in the calcium concentrations in cytosol and ER. The calcium dynamics of the cell become highly unstable for periodic electrical stimulation of the cell membrane and for periodic intracellular IP$_3$-mediated calcium oscillations.

Suppose that a cell in steady state without IP$_3$-mediated calcium oscillations (IP$_3$ concentration zero) is electrically stimulated such that it starts to generate action potentials. The inflow of calcium during the action potentials gives peaks in the calcium concentration in the cytosol (*upper left panel* of Fig. 5 *A*). The increased calcium concentration in the cytosol is reduced by activity of the PMCA and SERCA pumps. Since there is no release of calcium from the ER related to IP$_3$-mediated calcium oscillations, the activity of the SERCA pump after each action potential causes an accumulating increase of calcium in the ER (*dashed line* in *middle panel* of Fig. 5 *A*). With a constant leak of calcium through the plasma membrane (by choosing a constant value for the SOC conductance) the calcium concentration in the ER builds up to unrealistically high values in long-term runs.

However, introducing a SOC channel reduces the leak of calcium into the cytosol for high values of the calcium concentration in the ER (*solid line* in middle *panel* of Fig. 5 *A*). The reduced leak through the SOC channels causes a reduction in mean cytosolic calcium concentration and a reduction of SERCA activity. As a consequence, the averaged calcium concentration in the ER increases slightly.

Now suppose that there is no electrical stimulation, but that the cell is in a steady state with IP$_3$ equal to 0 μM, and then starts to produce IP$_3$-mediated calcium oscillations due to an increase of IP$_3$ concentration to 0.5 μM (Fig. 5 *B*). Each cycle of calcium release from the ER increases the calcium concentration in the cytosol, leading to opening of the calcium-dependent chloride channels and depolarization of the cell (*lower panel* in Fig. 5 *B*). The depolarization opens the L-type calcium channels, causing inflow of calcium through the membrane into the cytosol. As explained before (see Fig. 4, *D* and *E*), the inflow of calcium through the L-type calcium channels in this condition is approximately three-times smaller than in the case of electrical stimulation. Therefore, the large peak in the action potential up to +20 mV in Fig. 5 *A*, which is due to sudden simultaneous opening of all L-type calcium channels, is absent in Fig. 5 *B*. In the time periods between the IP$_3$-mediated calcium oscillations, both the PMCA and SERCA pump remove calcium from the cytosol. However, since the inflow of calcium from the extracellular space is relatively small, there is a net mean efflux of calcium out of the cell, decreasing the calcium concentration in the ER. If the leak of calcium through the cell membrane would be constant for all conditions, the consequence would be a depletion of calcium from the ER. This is illustrated in Fig. 5 *B* (*dashed line* in *middle panel*). After the rapid decrease of the calcium concentration in the ER, inactivation of the IP$_3$ receptor allows the SERCA pump to increase calcium in the ER. However, after some time the
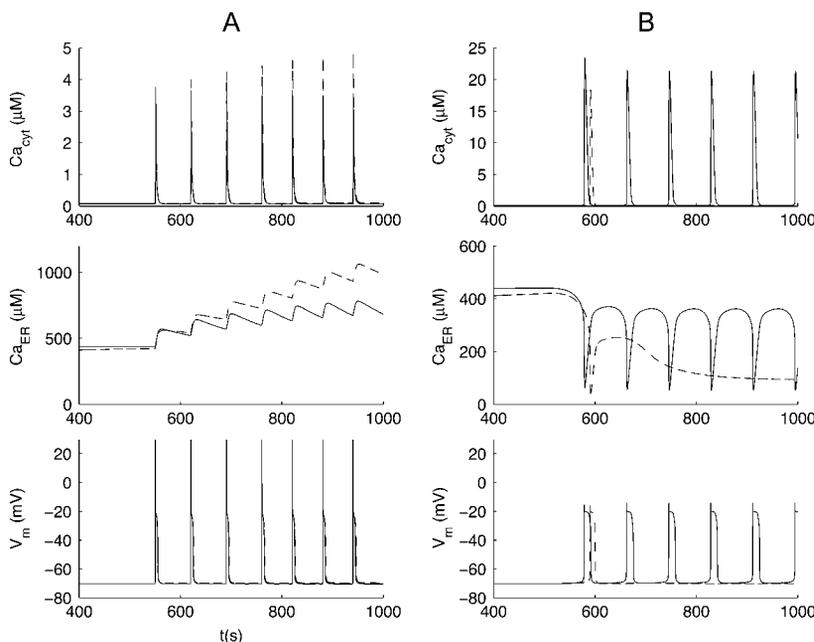

FIGURE 5 Simulation of the complete model with a constant SOC conductance value versus that with an ER-filling-dependent SOC conductance. Panel *A* shows the resting membrane potential (*lower panel*) and the steady state of the calcium concentration in the cytosol (*upper panel*) and in the ER (*middle panel*) for an IP$_3$ concentration of zero. At time 500 s, we induced action potentials (*APs*) (*lower panel*) and CaOs (*upper* and *middle panels*) by electrical current pulses, first with a constant SOC conductance value $((K_{\mathrm{SOC}}/(440 + K_{\mathrm{SOC}})))$ in the model (*dashed line*) and then with an ER-filling-dependent SOC conductance (Eq. 16) (*solid line*). Panel *B* shows the steady state of the calcium concentration in the cytosol (*upper panel*) and ER (*middle panel*) for an IP$_3$ concentration of zero until time 500 s. At time 500 s, the IP$_3$ concentration is changed to 0.5 μM. This will generate CaOs in the cytosol (*upper panel*) and in the ER (*middle panel*) and APs (*lower panel*) with implementation of Eq. 16 for the ER-dependent SOC conductance in the model (*solid line*) and one single CaO and AP with a constant SOC conductance (*dashed line*).

inactivation of the w-gate in the IP$_3$ receptor decays, allowing an inflow of calcium in the cytosol from the ER. Since the concentration of calcium in the ER is relatively small, the flow of calcium through the IP$_3$ receptor is much smaller than during the first calcium release. As a consequence, the f-gate, which depends on cytosolic calcium, opens gradually, leading to a small but continuous flow of calcium from the ER into the cytosol. This gives rise to a low calcium concentration in the ER (*dashed line* in *middle panel* of Fig. 5 *B*). However, if we add a SOC channel in the cell membrane, a decrease of calcium concentration in the ER leads to an increase of calcium inflow through the cell membrane in the cytosol (40). Since small changes in cytosolic calcium concentration lead to large changes in calcium concentration in the ER (8000 times larger), the presence of SOC channels prevents depletion of the ER (*solid line* in *middle panel*).

The main conclusion from Fig. 5 is that SOC channels can maintain a balance of calcium in the ER for both conditions of electrical stimulation and spontaneous IP$_3$-mediated calcium oscillations.

Notice the difference in the duration of the plateau phase in the lower panel of Fig. 5, *A* and *B*. Since the IP$_3$ concentration is zero in Fig. 5 *A*, it is not possible to open the IP$_3$ receptor and to initiate intracellular calcium oscillations. As a consequence, the peak value of the calcium concentration in the cytosol after an action potential is approximately a quarter of the peak value of the calcium concentration of the cytosol of a cell with IP$_3$ concentration above zero (see *upper panels* in Fig. 5). As a result, it takes less time for the PMCA and SERCA pump to reduce the calcium concentration in the cytosol to its basal concentration if the IP$_3$ concentration is zero. Since the duration of the plateau phase depends on the calcium con-

centration in the cytosol via the calcium-dependent chloride channels, the duration of the plateau phase of the APs is smaller in Fig. 5 *A* (*lower panel*) than in Fig. 5 *B*.

The calcium flux through the SOC channel has large implications for the cell behavior. This is illustrated in Fig. 6, which shows the behavior of the complete model for a fixed concentration IP$_3$ (0.5 μM) and with the conductance G_{SOC} increasing from 0 to 0.1 nS in steps of 0.025 nS (Fig. 6 *A*). Fig. 6 *B* shows the calcium concentration in the cytosol, Fig. 6 *C* the calcium concentration in the ER, and Fig. 6 *D* shows the membrane potential of the cell. For small values of G_{SOC}, the cytosolic calcium concentration is small and f_∞ (Eq. 26) is too small to open the IP$_3$ receptor (Fig. 6 *E*). When G_{SOC} increases, the cytosolic calcium concentration increases, leading to periodic opening and closing of the IP$_3$ receptor. Fig. 6 *E* shows the f-activation (*dashed-dotted line*) and w-inactivation parameter (*dotted line*) of the IP$_3$ receptor. The solid line shows the product of f and w. After each calcium oscillation, the inactivation gate w suddenly decreases and then gradually opens, causing an increase in the product fw and thereby causing the IP$_3$ receptor to leak calcium into the cytosol. This activates the f-gate of the IP$_3$ receptor and gives positive feedback to the IP$_3$ receptor. As a result, a calcium burst is released through the IP$_3$ receptor.

DISCUSSION

The aim of this study was to develop an integrated single-cell model for NRK cell excitability and intracellular calcium oscillations by combining a Hodgkin-Huxley type model for action-potential generation with a model for intracellular IP$_3$-mediated calcium oscillations. The present model is a
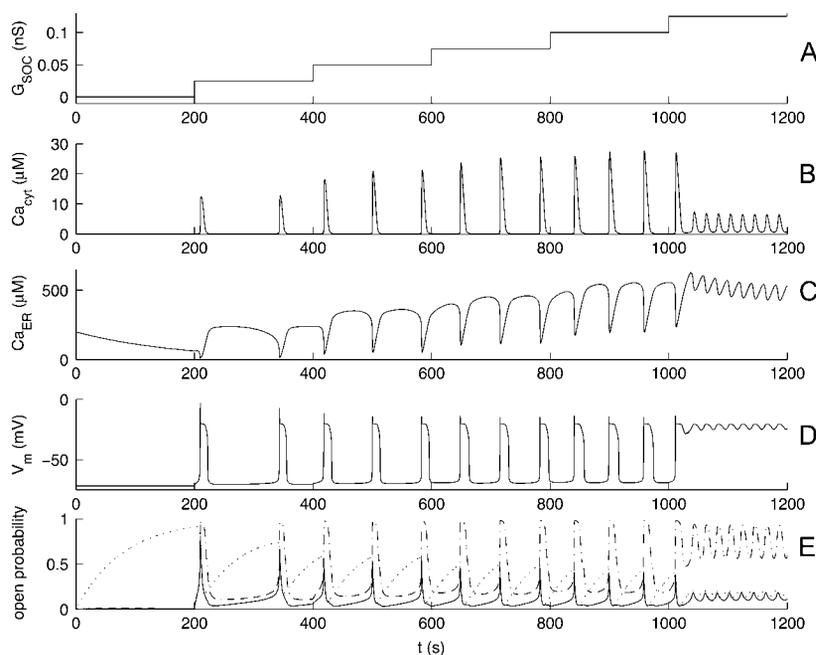

FIGURE 6 Simulation of the complete model with IP$_3$ = 0.5 μM and stepwise increasing G_{SOC} from 0 to 0.1 nS in steps of 0.025 nS. The figure shows the increase of G_{SOC} (*A*), the calcium concentration in the cytosol (*B*), the calcium concentration in the ER (*C*), and the membrane potential of the cell (*D*). When G_{SOC} increases above 0.125 nS, the level of calcium concentration in the cytosol increases and the membrane potential goes to -20 mV. Panel *E* shows the f-activation (*dashed-dotted line*) and w-inactivation (*dotted line*) parameter of the IP$_3$ receptor. The solid line shows the product of f and w. We chose a G_{SOC} value (0.05 nS) so that the cell oscillates and generates APs.

minimal model, containing the essential components to reproduce the qualitative electrical behavior and spontaneous calcium oscillations of NRK cells. Although the model was primarily developed to reconstruct calcium oscillations in NRK fibroblasts, the results have general applicability.

The new single-cell model revealed several new characteristics:

1. Combining a known AP model for the cell membrane with a model for intracellular calcium oscillations resulted in the instability of the calcium dynamics of the whole cell. Stability of the whole-cell behavior required a control system to keep the calcium concentration in cytosol and ER within certain limits. Here we show that this role can be fulfilled by store-operated calcium channels in the cell membrane. However, it is possible that other channels fulfill the same role, like diacylglycerol-activated (42) and arachidonate(ARC)-regulated Ca^{2+} channels (43) or reversible SERCA pumps (44).

2. There is a mutual influence between excitability of the plasma membrane and the IP_3-dependent calcium oscillator. Action-potential firing on the one hand may trigger IP_3-receptor-dependent intracellular calcium oscillations and on the other hand, intracellular calcium oscillations may induce rhythmic firing of chloride-mediated action potentials. The characteristics of the action potential, however, are different in the two conditions. These results will be discussed in more detail below in the context of available experimental data for NRK fibroblasts and the numerical model simulations of this study.

The involvement of the IP_3 receptor

Several mathematical models have been proposed in the literature for the IP_3 receptor (for an overview, see Schuster et al. (7)). Usually, two classes of models with intracellular calcium oscillations mediated by the IP_3 receptor are distinguished. The first class of models—called the Ca_{cyt}/IP_3 models; see, e.g., (29,45)—assume that the dynamics of the IP_3 receptor is determined by the concentrations of the cytoplasmic calcium and IP_3. The second class of models (Ca_{cyt}/Ca_{ER} models; see, e.g., (46,47)) assume that the dynamics of the IP_3 receptor is dependent on the calcium concentration in the cytosol as well as in the ER.

In this study we opted for the Li and Rinzel model (29). This choice was based on the different behavior of the two model types upon the frequency of the calcium oscillations affected by changes in SERCA pump activity. In the class of Ca_{cyt}/IP_3 models, an increased SERCA pump activity will have no effect on the frequency of the calcium oscillations, since the frequency of the calcium oscillations only depends on the time τ_w for the de-inactivation of the w-gate of the IP_3 receptor, which is determined by the IP_3 concentration.

For the class of Ca_{cyt}/Ca_{ER} models, the effect of increased SERCA pump activity is more complex. A typical model

from the Ca_{cyt}/Ca_{ER} class contains a factor proportional to $[Ca_{cyt}^{2+}]^4$ and a factor proportional to $[Ca_{cyt}^{2+}]^2$ and is represented by $J_{IP_3R} = ([Ca_{ER}^{2+}]^2/(Kr^2 + [Ca_{ER}^{2+}]^2))([Ca_{cyt}^{2+}]^4/([Ca_{cyt}^{2+}]^4 + K_A^4)) V_{IP_3}^{max}$ (see, e.g., (45)). The net flux of calcium from the ER to the cytosol is defined by the leak through the IP_3 receptor and a leak channel in the ER minus the removal of calcium into the ER by the SERCA pump. When the SERCA pump is more active, the net flux of calcium into the cytosol decreases. Therefore, it takes more time to increase the calcium concentration in the cytosol to open the activation gate to sufficiently high values to cause an IP_3-mediated calcium oscillation. This explains why the frequency of the calcium oscillations decreases with increased SERCA pump activity for the class of Ca_{cyt}/Ca_{ER} models.

Therefore, the main qualitative difference between the Ca_{cyt}/IP_3 and the Ca_{cyt}/Ca_{ER} models is that the former predict a constant oscillation frequency for IP_3-mediated calcium oscillations, whereas the latter predict lower oscillation frequencies when SERCA pump activity increases. In recent experiments, Harks et al. (19) showed that partial blocking of the SERCA pump with thapsigargin reduces the amplitude of the oscillations by ~30%, but does not affect the frequency of the oscillations. Based on these experimental findings, we decided to use the Ca_{cyt}/IP_3 model described by Li and Rinzel (29) (see Eq. 23), which is a reduced version of the De Young-Keizer model (30).

Recent preliminary real-time reverse transcriptase polymerase chain reaction studies in our laboratory revealed that the IP_3-receptor isoforms IP_3R1 and IP_3R3 are expressed in NRK cells, whereas the IP_3R2 isoform is not (W. Almirza, E. Zoelen, and A. Theuvenet, unpublished results). Interestingly, distinct roles of the IP_3R1 and IP_3R3 have been described in calcium signaling (48). In Hela cells expressing comparable amounts of IP_3R1 and IP_3R3, knockdown by RNA interference of each subtype resulted in dramatically distinct calcium signaling patterns. Knockdown of IP_3R1 significantly decreased total calcium signals and terminated calcium oscillations. Conversely, knockdown of IP_3R3 leads to more robust and long-lasting calcium oscillations than in controls, suggesting that IP_3R3 might function as an anti-calcium-oscillatory unit (48). Our finding that single isolated NRK fibroblasts can be induced to respond with intracellular calcium oscillations (see Fig. 7 A; see Appendix 1) upon exposure to $PGF_{2\alpha}$, therefore, supports our model assumption of the involvement of IP_3R1 in calcium oscillations, and justifies the use of its kinetic features in modeling the intracellular calcium oscillator. In this minimal model we have not included features of IP_3R3. The involvement of specifically IP_3R1 is further supported by the finding that thimerosal (recently shown to potentiate IP_3-dependent calcium fluxes through IP_3R1, but not the type-3 receptor, via modulation of an isoform-specific calcium-dependent intramolecular interaction (41)) indeed amplifies the $PGF_{2\alpha}$-induced calcium response of an initially poorly responding cell (Fig. 7 B and Appendix 1).

Intracellular calcium buffering and compartmentalization

The characteristics of the calcium oscillations of the whole cell model are strongly dependent on the parameters of the calcium buffer in the cytosol. Changing the buffer parameters affects the calcium concentration in the cytosol and the duration of the plateau phase. The duration of the plateau depends on the activity of the calcium-dependent chloride channels. When the calcium concentration in the cytosol decreases due to a higher affinity (k_{on}) and/or due to an increase of total buffer capacity T_B, the calcium-dependent chloride channel will close earlier with the consequence that the duration of the plateau phase becomes shorter. The precise buffering properties for calcium in NRK cells are not known. In the membrane model of Torres et al. (18), the values of the buffer parameters were different from the parameters in this model. This is mainly due to the fact that simulations of Torres et al. (18) were aimed to reproduce experimental results in conditions of non-natural calcium buffers like EGTA and BAPTA.

The peak values of the calcium concentration in the cytosol during an oscillation are much higher than reported in the literature (see, e.g., (32)). Theoretical models and indirect experimental observations have predicted that calcium concentrations at the inner surface of the plasma membrane reach, upon stimulation, values much higher than those of the bulk cytosol. Marsault et al. (49) demonstrated that the mean calcium concentration near the plasma membrane can reach values >10-fold higher than those of the bulk cytosol upon activation of calcium influx through plasma membrane channels. Our explanation for the high calcium concentration in the model is the simplification of intracellular calcium dynamics by the absence of intracellular compartmentalization. If the cytosol is considered as a finite volume with diffusion of calcium ions in the cytosol, the average concentration of calcium ions in the cytosol will be much lower than that near the membrane (in case of an action potential) or near the ER (for IP$_3$-mediated calcium oscillations).

The importance of feedback of ER filling to calcium inflow transporters

The calcium concentration in the store depends critically on the ratio of the activity of the SERCA pump and the leak of calcium through the ER membrane. For a cell at rest, it is possible to choose the parameters for the plasma membrane calcium (PMCA) pump, the SERCA pump, Ca^{2+}-leak channels through the plasma membrane, and Ca^{2+}-leak channels through the ER membrane such that a stable situation occurs. However, this stability at rest is lost when action potentials or IP$_3$ oscillations lead to changes in the Ca^{2+} concentration of the cytosol.

This instability could be overcome by introducing a channel controlled by feedback of the store, which provides a coupling between the calcium currents through the cell membrane and the calcium concentration in the ER—for example, a store-operated calcium channel (SOC). The existence of SOCs is well known and well accepted. Recent experimental findings have shown that calcium entry through SOC channels is essential to sustain receptor-induced intracellular calcium oscillations (50). In nonexcitable cells, they provide the most important calcium influx in the cytosol (51), and thereby regulate the calcium concentration in the ER via the calcium concentration in the cytosol. Activation of SOCs is triggered by depletion of intracellular calcium stores. Despite the intense research in the field, the mechanism that links the fall of calcium concentration in the stores to the opening of plasma membrane calcium channels remains highly controversial. One set of hypotheses postulates the release of a diffusible messenger by the pools, while others claim a physical interaction between the empty stores and plasma membrane involving membrane proteins, secretory vesicles, and possibly cytoskeletal elements (reviewed in (52,53)).

Although SOC channels in NRK fibroblasts have not yet been demonstrated experimentally, their expression in these cells seems most likely. In NRK fibroblasts the induction of calcium oscillations by PGF$_{2\alpha}$ is not affected by blockers of L-type calcium channels but is prevented in calcium-free extracellular media (19). These findings thus agree with the model prediction that stable long-term CaOs require influx of extracellular calcium mediated by a plasma membrane channel, other than the L-type calcium channel, possibly a SOC channel. In our model simulations we found that stable calcium dynamics could be achieved with values for a whole-cell SOC conductance (G_{SOC}) near 0.05 nS. These values are of the same order of magnitude as experimentally determined by Rychkov et al. (13) for a SOC channel in rat hepatocytes.

Some other channels may very well regulate the calcium dynamics in a similar way. The central idea is that there has to be some feedback of ER calcium content upon cytosolic calcium entry. Falcke et al. (54), Chay (10), and Li et al. (12) discuss models for stable calcium dynamics without a store-operated channel. Their mechanism is based on a calcium-dependent K^+ current. These channels could be useful to control a stable long-term operation of the cell. However, the presence of calcium-dependent potassium channels in our NRK cell can be excluded for three reasons:

1. Ion-substitution experiments revealed that the calcium-dependent current in voltage-clamp experiments was a chloride current (17).
2. Current-clamp measurements show that an increased PGF$_{2\alpha}$ agonist concentration leads to an increased intracellular calcium concentration and a depolarization of membrane potential toward the Nernst potential of chloride channels (17). The presence of a calcium-dependent K-channel would result in a hyperpolarization, consistent with the model by Loewenstein et al. (21).

3. Charybdotoxin blocks certain calcium-dependent potassium channels, but this blocker has no effect on the membrane potential of NRK cells during IP$_3$-mediated calcium oscillations (personal communication with E. G. Harks). Therefore, a different mechanism should be involved in our NRK cells. Sneyd et al. (14) suggested a modification of the SERCA-pump dynamics to control the balance of calcium ions in the cytosol and the ER, such that lower concentrations of calcium in the ER lead to higher activity of the SERCA pump. An SOC channel and the modified SERCA dynamics, used by Sneyd et al. (14), have the same qualitative effect on the regulation of the total amount of calcium in the ER. However, there is a small difference between the modified SERCA pump and the SOC channel. If the concentration of calcium in the ER is suddenly decreased, the modified SERCA pump will become more active, leading to a decrease of calcium in the cytosol. In contrast to that, a decrease in the calcium concentration in the ER leads to an initial increase of [Ca$_{cyt}^{2+}$] for a cell model with SOC channels in the membrane.

One of the main criticisms regarding the store-operated calcium channels in the plasma membrane concerned the signaling mechanism that senses Ca^{2+} store depletion and triggers opening of the store-operated calcium channel. Recently, it was shown (55,56) that the stromal interaction molecule (STIM) acts as the missing link between store and plasma membrane. This finding supports the presence of store-operated channels and fits very well with the important function of store-operated channels that is postulated in our study.

APPENDIX 1: CALCIUM OSCILLATIONS IN SINGLE NRK CELLS

The basic property of the present NRK-cell model is that it is able to generate self-sustained IP$_3$-dependent intracellular calcium oscillations. This property is based on our previous work (16), where we found good evidence that NRK cells in a monolayer culture under certain conditions are able to generate spontaneous intracellular IP$_3$-mediated calcium oscillations, independent of the neighbor cells to which they are coupled by gap junctions. To further support this idea, we addressed the question of whether the exhibition of prolonged intracellular calcium oscillations is an intrinsic property of a single NRK fibroblast in isolation, or instead requires, for some reason, gap-junctional coupling of the cell to other cells in a network of electrically or chemically coupled cells. For that purpose we measured the calcium response of single, isolated Fura-2-loaded NRK fibroblasts upon exposure to PGF$_{2\alpha}$, because this prostaglandin was able to induce IP$_3$-dependent calcium oscillations in NRK-monolayer cells (16).

Quiescent monolayers of normal rat kidney fibroblasts (NRK clone 49F) were cultured and dissociated in single cells by trypsinization as described previously (17). The experiments on the dissociated cell cultures were performed 2–4 h after trypsinization when NRK cells had been sufficiently attached to the culture dish. Intracellular calcium measurements were as described in detail in Harks et al. (19): Coverslips with trypsinized single NRK fibroblasts in isolation were placed in a cell chamber and loaded with Fura-2/AM. Dynamic video imaging was performed as described elsewhere (24). Excitation wavelengths were 340 nm and 380 nm and Fura-2 fluorescence

emission was monitored at wavelengths above 440 nm. Ratio images (F340/F380) were calculated every 6 s and plotted as a function of time to monitor relative changes in the cytosolic [Ca^{2+}] (see Fig. 7).

As in our previous studies on monolayers of gap-junctionally coupled NRK cells (19), 1 μM PGF$_{2\alpha}$ induced calcium responses in individual cells in a population of single NRK fibroblasts in isolation. The trypsinized single, isolated NRK fibroblasts appeared less responsive to exposure to 1 μM PGF$_{2\alpha}$ than the NRK cells in the intact monolayer culture. In an imaged area of the coverslip, three of 26 cells showed an initial large calcium transient followed by prolonged calcium oscillations (Fig. 7 A) with similar shapes and frequencies (0.2–1.4 min^{-1}) as induced in monolayer cells (19).

The remainder of the isolated single cells only showed the initial large calcium transient upon exposure to PGF$_{2\alpha}$ sometimes followed by a second delayed transient. However, in a field of 14 of these single initial-peak responders imaged, 13 cells started sustained calcium oscillations upon exposure to 10-μM thimerosal (Fig. 7 B), a compound that has been described to sensitize the type-1 IP$_3$ receptor (41). Thimerosal (10 μM), even without prior exposure of the cells to PGF$_{2\alpha}$, already induced calcium oscillations in these cells with a comparable delay ($n = 10$, data not shown). A plausible interpretation of these observations is that the direct oscillation responders to PGF$_{2\alpha}$ could serve as pacemaker cells in a periodically firing NRK-monolayer culture, whereas the initial-peak responders could behave as follower cells. In summary, we conclude that at least a percentage of single, isolated NRK cells has the intrinsic property to generate sustained IP$_3$-dependent calcium oscillations. This percentage is probably an
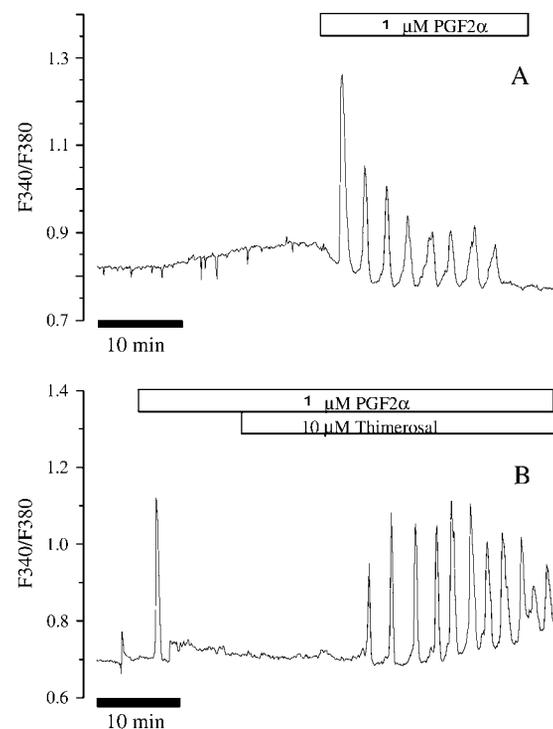

FIGURE 7 Induction of calcium oscillations in single isolated NRK fibroblasts by PGF$_{2\alpha}$. (A) Example of a cell exhibiting PGF$_{2\alpha}$-induced calcium oscillations characterized by an initial sharp calcium peak resulting from calcium release from IP$_3$-sensitive stores, which was followed by a secondary response consisting of prolonged repetitive calcium oscillations, comparable to those described for cells in monolayer cultures by Harks et al. (16). (B) An example of a poorly responding cell showing only the initial calcium transient. Subsequent addition of 10 μM thimerosal amplified the PGF$_{2\alpha}$-induced calcium response of this cell, as shown by the delayed appearance of secondary repetitive calcium oscillations.

underestimate because of the experimental conditions (trypsinization). Thus, the property that the single NRK-cell model can generate self-sustained IP$_3$-dependent calcium oscillations is supported by ample experimental evidence.

APPENDIX 2: EQUATIONS

The equations defining the electrical membrane properties of NRK fibroblastic cells and associated intracellular calcium buffering, unconnected to the intracellular calcium model (for explanations, see text and Table 1):

$$C_m \frac{dV_m}{dt} = -(I_{Kir} + I_{lk} + I_{CaL} + I_{Cl(Ca)} + I_{SOC}), \quad (1)$$

$$I_{Kir} = G_{Kir} \sqrt{\frac{K_o}{K_{ost}}} \left(\frac{\alpha}{\alpha + \beta}\right)(V_m - E_K), \quad (2)$$

$$\alpha = \frac{0.1}{1 + \exp[0.06(V_m - E_K - 50)]}, \quad (3)$$

$$\beta = \frac{3\exp[0.0002(V_m - E_K + 100)] + \exp[0.0002(V_m - E_k - 10)]}{1 + \exp[-0.06(V_m - E_K - 50)]}, \quad (4)$$

$$E_K = 1000 \frac{RT}{F} \ln\left(\frac{K_o}{K_i}\right), \quad (5)$$

$$I_{lk} = G_{lk}(V_m - E_{lk}), \quad (6)$$

$$I_{CaL} = m\,h\,v_{Ca}\,G_{CaL}\,(V_m - E_{CaL}), \quad (7)$$

$$\frac{dm}{dt} = \frac{m_\infty - m}{\tau_m}, \quad (8)$$

$$m_\infty = \frac{1}{1 + \exp\left(-\frac{V_m + 15}{5.24}\right)}, \quad (9)$$

$$\tau_m = 0.01 \frac{m_\infty (1 - \exp(-(V_m + 10)/5.9))}{0.035(V_m + 10)}, \quad (10)$$

$$\frac{dh}{dt} = \frac{h_\infty - h}{\tau_h}, \quad (11)$$

$$h_\infty = \frac{1}{1 + \exp\left(\frac{V_m + 37}{4.6}\right)}, \quad (12)$$

$$\tau_h = \frac{0.01}{0.02 + 0.0197\exp(-[0.0337(V_m + 10)]^2)}, \quad (13)$$

$$v_{Ca} = \frac{K_{vCa}}{\left[Ca^{2+}_{cyt}\right] + K_{vCa}}, \quad (14)$$

$$I_{Cl(Ca)} = \frac{\left[Ca^{2+}_{cyt}\right]}{\left[Ca^{2+}_{cyt}\right] + K_{Cl(Ca)}} G_{Cl(Ca)}(V_m - E_{Cl(Ca)}), \quad (15)$$

$$I_{SOC} = \frac{K_{SOC}}{\left[Ca^{2+}_{ER}\right] + K_{SOC}} G_{SOC}(V_m - E_{SOC}), \quad (16)$$

$$Vol_{cyt} \frac{d\left[Ca^{2+}_{cyt}\right]}{dt} = -Vol_{cyt} \frac{d[BCa]}{dt} + A_{PM} J_{PM} \quad (17)$$

$$\frac{d[BCa]}{dt} = k_{on}([T_B] - [BCa])\left[Ca^{2+}_{cyt}\right] - k_{off}[BCa], \quad (18)$$

$$J_{PM} = -\frac{10^{-6}}{z_{Ca}F} \frac{1}{A_{PM}}(I_{CaL} + I_{SOC}) - J_{PMCA}, \quad (19)$$

$$J_{PMCA} = J_{PMCA}^{max} \frac{\left[Ca^{2+}_{cyt}\right]}{\left[Ca^{2+}_{cyt}\right] + K_{PMCA}}. \quad (20)$$

The equations defining the properties of the intracellular calcium dynamics model of NRK cells isolated from the electrical membrane model when J_{PM} is zero (see Eq. 19):

$$Vol_{cyt} \frac{d\left[Ca^{2+}_{cyt}\right]}{dt} = A_{ER}(J_{IP_3R} + J_{lkER} - J_{SERCA}) - \frac{d[BCa]}{dt} Vol_{cyt} + A_{PM} J_{PM}, \quad (21)$$

$$Vol_{ER} \frac{d\left[Ca^{2+}_{ER}\right]}{dt} = A_{ER}(-J_{IP_3R} - J_{lkER} + J_{SERCA}), \quad (22)$$

$$J_{IP_3R} = f_\infty^3 w^3 K_{IP_3R} \left(\left[Ca^{2+}_{ER}\right] - \left[Ca^{2+}_{cyt}\right]\right), \quad (23)$$

$$J_{lkER} = K_{lkER}\left(\left[Ca^{2+}_{ER}\right] - \left[Ca^{2+}_{cyt}\right]\right), \quad (24)$$

$$J_{SERCA} = J_{SERCA}^{max} \frac{\left[Ca^{2+}_{cyt}\right]^2}{K_{SERCA}^2 + \left[Ca^{2+}_{cyt}\right]^2}, \quad (25)$$

$$f_\infty = \frac{\left[Ca^{2+}_{cyt}\right]}{K_{fIP_3} + \left[Ca^{2+}_{cyt}\right]}, \quad (26)$$

$$\frac{dw}{dt} = \frac{w_\infty - w}{\tau_w}, \quad (27)$$

$$w_\infty = \frac{\frac{[IP_3]}{K_{wIP_3} + [IP_3]}}{\frac{[IP_3]}{K_{wIP_3} + [IP_3]} + K_{w(Ca)}\left[Ca^{2+}_{cyt}\right]}, \quad (28)$$

$$\tau_{\text{w}} = \frac{a}{\dfrac{[\text{IP}_3]}{K_{\text{wIP}_3} + [\text{IP}_3]} + K_{\text{w(Ca)}}\left[\text{Ca}^{2+}_{\text{cyt}}\right]}. \qquad (29)$$

REFERENCES

1. Ramirez, J. M., A. K. Tryba, and F. Peña. 2004. Pacemaker neurons and neuronal networks: an integrative view. *Curr. Opin. Neurobiol.* 14:665–674.

2. Stojilkovic, S. S., M. Kukuljan, T. Iida, E. Rojas, and K. J. Catt. 1992. Integration of cytoplasmic calcium and membrane potential oscillations maintains calcium signaling in pituitary gonadotrophs. *Proc. Natl. Acad. Sci. USA.* 89:4081–4085.

3. LeBeau, A. P., D. I. Yule, G. E. Groblewski, and J. Sneyd. 1999. Agonist-dependent phosphorylation of the inositol 1,4,5-trisphos-phate receptor: a possible mechanism for agonist-specific calcium oscillations in pancreatic acinar cells. *J. Gen. Physiol.* 113:851–872.

4. Ward, S. M., T. Ordog, S. D. Koh, S. Abu Baker, J. Y. Jun, G. Amberg, K. Monaghan, and K. M. Sanders. 2000. Pacemaking in interstitial cells of Cajal depends upon calcium handling by endo-plasmic reticulum and mitochondria. *J. Physiol.* 525:355–361.

5. Hodgkin, A. L., and A. Huxley. 1952. A quantitative description of the membrane current and its application to conduction and excitation in nerve. *J. Physiol.* 117:500–544.

6. Koch, C. 1999. Biophysics of Computation, Information Processing in Single Neurons, 1st Ed. Oxford University Press, Oxford, UK.

7. Schuster, S., M. Marhl, and T. Höfer. 2002. Modelling of simple and complex calcium oscillations. from single-cell response to intercellular signalling. *Eur. J. Biochem.* 269:1333–1355.

8. Sneyd, J., and M. Falcke. 2005. Models of inositol trisphosphate receptor. *Prog. Biophys. Mol. Biol.* 89:207–245.

9. Falcke, M. 2004. Reading the patterns in living cells—the physics of Ca^{2+} signaling. *Adv. Phys.* 53:255–440.

10. Chay, T. 1996. Electrical bursting and luminal calcium oscillation in excitable cell models. *Biol. Cybern.* 75:419–431.

11. Keizer, J., and G. De Young. 1993. Effect of voltage-gated plasma membrane Ca^{2+} fluxes on IP_3-linked Ca^{2+} oscillations. *Cell Calcium.* 14:397–410.

12. Li, Y. X., S. S. Stojilkovic, J. Keizer, and J. Rinzel. 1997. Sensing and refilling calcium stores in an excitable cell. *Biophys. J.* 72:1080–1091.

13. Rychkov, G. Y., T. Litjens, M. L. Roberts, and G. J. Barritt. 2005. ATP and vasopressin activate a single type of store-operated Ca^{2+} channel, identified by patch-clamp recording, in rat hepatocytes. *Cell Calcium.* 37:183–191.

14. Sneyd, J., K. Tsaneva-Atanasova, D. I. Yule, J. L. Thompson, and T. J. Shuttleworth. 2004. Control of calcium oscillations by membrane fluxes. *Proc. Natl. Acad. Sci. USA.* 101:1392–1396.

15. de Roos, A. D., P. H. Willems, P. H. Peters, E. J. van Zoelen, and A. P. Theuvenet. 1997. Synchronized calcium spiking resulting from spontaneous calcium action potentials in monolayers of NRK fibroblasts. *Cell Calcium.* 22:195–207.

16. Harks, E. G., P. H. Peters, J. L. van Dongen, E. J. van Zoelen, and A. P. Theuvenet. 2005. Autocrine production of prostaglandin $F_{2\alpha}$ enhances

17. Harks, E. G., J. J. Torres, L. N. Cornelisse, D. L. Ypey, and A. P. Theuvenet. 2003. Ionic basis for excitability in normal rat kidney (NRK) fibroblasts. *Am. J. Physiol. Cell Physiol.* 196:493–503.

18. Torres, J. J., L. N. Cornelisse, E. G. A. Harks, W. P. M. van Meerwijk, A. P. R. Theuvenet, and D. L. Ypey. 2004. Modeling action potential generation and propagation in NRK fibroblasts. *Am. J. Physiol. Cell Physiol.* 287:C851–C865.

19. Harks, E. G., W. J. Scheenen, P. H. Peters, E. J. van Zoelen, and A. P. Theuvenet. 2003. Prostaglandin $F_{2\alpha}$ induces unsynchronized intracellular calcium oscillations in monolayers of gap junctionally coupled NRK fibroblasts. *Pflugers Arch.* 447:78–86.

20. Harks, E. G. 2003. Excitable fibroblast! Ion channels, gap junctions, action potentials and calcium oscillations in normal rat kidney fibroblasts. PhD thesis. Raboud University, Nijmegen, The Netherlands.

21. Loewenstein, Y., Y. Yarom, and H. Sompolinsky. 2001. The generation of oscillations in networks of electrically coupled cells. *Proc. Natl. Acad. Sci. USA.* 98:8095–8100.

22. Rorsman, P., and G. Trube. 1986. Calcium and delayed potassium currents in mouse pancreatic β-cells under voltage-clamp conditions. *J. Physiol.* 374:531–550.

23. Valdeolmillos, M., A. Gomis, and J. V. Sanchez-Andres. 1996. In vivo synchronous membrane potential oscillations in mouse pancreatic β-cells: lack of coordination between islets. *J. Physiol.* 493:9–18.

24. Cornelisse, L., R. Deumens, J. J. A. Coenen, E. W. Roubos, C. C. A. M. Gielen, D. L. Ypey, B. G. Jenks, and W. J. J. M. Scheenen. 2002. Sauvagine regulates Ca^{2+} oscillations and electrical membrane activity of melanotrope cells of *Xenopus laevis*. *J. Neuroendocrinol.* 14: 77–78.

25. Caride, A. J., A. R. Penheiter, A. G. Filoteo, Z. Bajzer, A. Enyedi, and J. T. Penniston. 2001. The plasma membrane calcium pump displays memory of past calcium spikes. Differences between isoforms 2b and 4b. *J. Biol. Chem.* 276:39797–39804.

26. Bernus, O., R. Wilders, C. W. Zemlin, H. Verschelde, and A. V. Panfilov. 2002. A computationally efficient electrophysiological model of human ventricular cells. *Am. J. Physiol. Heart Circ. Physiol.* 282: H2296–H2308.

27. ten Tusscher, K. H. W. J., D. Noble, P. J. Noble, and A. V. Panfilov. 2004. A model for human ventricular tissue. *Am. J. Physiol. Heart Circ. Physiol.* 286:H1573–H1589.

28. Prakriya, M., and R. S. Lewis. 2003. CRAC channels: activation, permeation, and the search for a molecular identity. *Cell Calcium.* 33: 311–321.

29. Li, Y. X., and J. Rinzel. 1994. Equations for $InsP_3$ receptor-mediated $[Ca^{2+}]$ oscillations derived from a detailed kinetic model: a Hodgkin-Huxley like formalism. *J. Theor. Biol.* 166:461–473.

30. De Young, G. W., and J. Keizer. 1992. A single-pool inositol 1,4,5-trisphosphate-receptor-based model for agonist-stimulated oscillations in Ca^{2+} concentration. *Proc. Natl. Acad. Sci. USA.* 89:9895–9899.

31. Finch, E. A., T. J. Turner, and S. M. Goldin. 1991. Calcium as a coagonist of inositol 1,4,5-trisphosphate-induced calcium release. *Science.* 252:443–446.

32. Mak, D. O., S. McBride, and J. K. Foskett. 1998. Inositol 1,4,5-trisphosphate activation of inositol trisphosphate receptor Ca^{2+} channel by ligand tuning of Ca^{2+} inhibition. *Proc. Natl. Acad. Sci. USA.* 95: 15821–15825.

33. Mak, D. O., and J. K. Foskett. 1997. Single-channel kinetics, inactivation, and spatial distribution of inositol trisphosphate (IP_3) receptors in *Xenopus* oocyte nucleus. *J. Gen. Physiol.* 109:571–587.

34. Marchant, J. S., and C. W. Taylor. 1998. Rapid activation and partial inactivation of inositol trisphosphate receptors by inositol trisphoshate. *Biochemistry.* 37:11524–11533.

35. Dufour, J.-F., I. M. Arias, and T. J. Turner. 1997. Inositol 1,4,5-trisphosphate and calcium regulate the calcium channel function of the

hepatic inositol 1,4,5-trisphosphate receptor. *J. Biol. Chem.* 274:2675–2681.

36. Yule, D. I., S. V. Straub, and J. I. E. Bruce. 2003. Modulation of Ca^{2+} oscillations by phosphorylation of Ins(1,4,5)P$_3$ receptors. *Biochem. Soc. Trans.* 31:954–957.

37. Nash, M. S., K. W. Young, R. A. J. Challiss, and S. R. Nahorski. 2001. Intracellular signalling. Receptor-specific messenger oscillations. *Nature.* 413:381–382.

38. Lytton, J., M. Westlin, S. E. Burk, G. E. Shull, and D. H. MacLennan. 1992. Functional comparisons between isoforms of the sarcoplasmic or endoplasmic reticulum family of calcium pumps. *J. Biol. Chem.* 267:14483–14489.

39. Nägerl, U., D. Novo, I. Mody, and J. L. Vergara. 2000. Binding kinetics of calbindin-D(28k) determined by flash photolysis of caged Ca^{2+}. *Biophys. J.* 79:3009–3018.

40. Hofer, A. M., C. Fasolato, and T. Pozzan. 1998. Capacitative Ca^{2+} entry is closely linked to the filling state of internal Ca^{2+} stores: a study using simultaneous measurements of I_{CRAC} and intraluminal (Ca^{2+}). *J. Cell Biol.* 140:325–334.

41. Bultynck, G., K. Szlufcik, N. N. Kasri, Z. Assefa, G. Callewaert, L. Missiaen, J. B. Parys, and H. De Smedt. 2004. Thimerosal stimulates Ca^{2+} flux through inositol 1,4,5-trisphosphate receptor type 1, but not type 3, via modulation of an isoform-specific Ca^{2+}-dependent intramolecular interaction. *Biochem. J.* 381:87–96.

42. Hofmann, T., A. G. Obukhov, M. Schaefer, C. Harteneck, T. Gudermann, and G. Schultz. 1999. Direct activation of human TRPC6 and TRPC3 channels by diacylglycerol. *Nature.* 397:259–263.

43. Mignen, O., J. L. Thompson, and T. J. Shuttleworth. 2003. Calcineurin directs the reciprocal regulation of calcium entry pathways in non-excitable cells. *J. Biol. Chem.* 278:40088–40096.

44. MacLennan, D. H., W. J. Rice, and N. M. Green. 1997. The mechanism of Ca^{2+} transport by sarco(endo)plasmic reticulum Ca^{2+}-ATPases. *J. Biol. Chem.* 272:28815–28818.

45. Keizer, J., and G. De Young. 1994. Simplification of a realistic model of IP$_3$-induced Ca^{2+} oscillations. *J. Theor. Biol.* 166:431–442.

46. Torres, J. J., P. H. G. M. Willems, H. J. Kappen, and W. J. H. Koopman. 2001. Hysteresis and bistability in a realistic model for IP$_3$-driven Ca^{2+} oscillations. *Europhys. Lett.* 55:746–752.

47. Dupont, G., and A. Goldbeter. 1993. One-pool model for Ca^{2+} oscillations involving Ca^{2+} and inositol 1,4,5-trisphosphate as co-agonists for Ca^{2+} release. *Cell Calcium.* 14:311–322.

48. Hattori, M., A. Z. Suzuki, T. Higo, H. Miyauchi, T. Michikawa, T. Nakamura, T. Inoue, and K. Mikoshiba. 2004. Distinct roles of inositol 1,4,5-trisphosphate receptor types 1 and 3 in Ca^{2+} signaling. *J. Biol. Chem.* 279:11967–11975.

49. Marsault, R., M. Murgia, T. Pozzan, and R. Rizzuto. 1997. Domains of high Ca^{2+} beneath the plasma membrane of living A7r5 cells. *EMBO J.* 16:1575–1581.

50. Bird, G. S., and J. W. J. Putney. 2005. Capacitative calcium entry supports calcium oscillations in human embryonic kidney cells. *J. Physiol.* 562:697–706.

51. Putney, J. W. J. 1990. Capacitive calcium entry revisited. *Cell Calcium.* 11:611–624.

52. Putney, J. W. J., and R. McKay. 1990. Capacitive calcium entry channels. *Bioessays.* 21:38–46.

53. Parekh, A. B. 2003. Store-operated Ca^{2+} entry: dynamic interplay between endoplasmic reticulum, mitochondria and plasma membrane. *J. Physiol.* 547:333–348.

54. Falcke, M., R. Huerta, M. I. Rabinovich, H. D. I. Abarbanel, R. C. Elson, and A. I. Selverston. 2000. Modeling observed chaotic oscillations in bursting neuron: the role of calcium dynamics and IP$_3$. *Biol. Cybern.* 82:517–527.

55. Liou, J., M. L. Kim, W. Do Heo, J. T. Jones, J. W. Myers, J. E, J. Ferrell, and T. Meyer. 2005. STIM is a Ca^{2+} sensor essential for Ca^{2+}-store-depletion-triggered Ca^{2+} influx. *Curr. Biol.* 15:1235–1241.

56. Roos, J., P. J. DiGregorio, A. V. Yeromin, K. Ohlsen, M. Lioudyno, S. Zhang, O. Safrina, J. Ashot Kozak, S. L. Wagner, M. Cahalan, G. Velicelebi, and K. A. Stauderman. 2005. STIM1, an essential and conserved component of store-operated Ca^{2+} channel function. *J. Cell Biol.* 169:435–445.